Received: 5 September 2023 | Revised: 3 November 2023 | Accepted: 3 November 2023 | Published online: 13 November 2023

RESEARCH ARTICLE

Journal of Optics and Photonics Research
2024, Vol. 00(00) 1–6
DOI: 10.47852/bonviewJOPR32021689

BON VIEW PUBLISHING

Magnetic Field Sensor Using the Magnetic Fluid-Encapsulated Long-Period Fiber Grating Inscribed in the Thin-Cladding Fiber

Hua Wang[1,*], Qun He[1], Shuai Yuan[1], Wei Zeng[1], Yang Zhou[1], Ruchao Tan[1], Xiaolong Fan[2], Yuehui Ma[2] and Yu Zhu[2]

[1]*State Grid Jiangxi Information & Telecommunication Company, China*

[2]*Key Laboratory of Specialty Fiber Optics and Optical Access Network, Shanghai University, China*

Abstract: Optical magnetic field current sensors could overcome the shortcomings of traditional sensors based on electrical principles, such as large volume, insufficient sensitivity, and limitations of working environment, which can be applied to medical, military, and other fields with higher sensing requirements. We demonstrated experimentally the inscription of the long-period fiber gratings (LPFGs) in the thin-cladding fiber (TCF). The magnetic field current sensor is fabricated by encapsulating the TCF–LPFG with magnetic fluid (MF) nanoparticles. The principle of the sensor is based on the refractive index tunability of the MF with the magnetic field (current). The measurement of the external magnetic field (current) can be obtained by detecting the wavelength shift of the coated TCF–LPFG, which changes with the applied magnetic field. In the intensity range of 0 ∼ 11 mT, the experimental sensitivity of magnetic field measurement is up to −0.31 nm/mT. The proposed magnetic field current sensor has potential applications in practical measurement of magnetic field.

Keywords: long-period fiber gratings, electrical current, magnetic fluid, thin-cladding fiber

1. Introduction

The research and applications of the magnetic field sensors have attracted much attention in broadband areas. The magnetic field sensors using the traditional techniques are mainly used in the mobile phone and automotive industries, which are generally based on the principles of electrical effects, such as Hall effect [1], Faraday effect [2], and nuclear magnetic resonance [3]. Conventional electrical magnetic field sensors tend to have these drawbacks: difficult size reduction, high energy consumption, small measurement range, expensive cost, and harsh operating environment requirements [4]. Optical magnetic field sensors, however, can be applied to more demanding devices in biology, medicine, and military because of their advantages of small size, light weight, corrosion resistance, strong resistance to electromagnetic interference, and higher sensitivity [5–8]. Based on the principle of operation, optical magnetic field sensors could be further classified into magnetostrictive sensors, Faraday effect-based sensors, and magnetic fluid (MF)-based sensors [9–13]. Among them, the advantages of the MF-based optical sensors are more obvious with the rapid developing of nanomaterial technology. MF is an important nanomaterial, which is composed of colloidal magnetic nanoparticles that are highly stable and colloidal magnetic nanoparticles distribute in a suitable carrier liquid uniformly [14, 15]. MFs are rich in magneto-optical properties [16], such as Faraday effect, and refractive index (RI) tunability that varies with applied magnetic field.

Optical magnetic field sensors using MFs with fiber technologies usually include the following two types. One is to combine with the micro-structured fibers such as photonic crystal fibers (PCFs) to fill them with MF [17], the other is to realize the sensing measurement based on the fiber sensor head, which is sensitive to the RI variations induced by the surrounding MF [18]. For second scheme, the RI of the MF nanoparticles will alter in response to variations in the applied magnetic field's intensity. Therefore, the interaction of evanescent field of the coupled fiber cladding mode and MF can be adopted for the measurement of the magnetic field. The evanescent field coupling can be realized by different components such as tapered fiber, long-period fiber grating (LPFG), and D-shape fiber. The LPFG is a passive component, which can be designed to couple the light from fundamental LP_{01} mode to high order cladding modes. The MF-coated LPFG optical magnetic field sensors have a promising future application, thanks to the high RI sensitivity of the cladding modes and RI tunability of the MFs.

*Corresponding author: Hua Wang, State Grid Jiangxi Information & Telecommunication Company, China. The research was conducted at State Grid Jiangxi Information & Telecommunication Company, China. Correspondence concerning this article should be addressed to wzh_hf@163.com

Figure 1
(a) RI distribution of TCF cross-section. (b) The CCD diagram of splicing between TCF and SMF

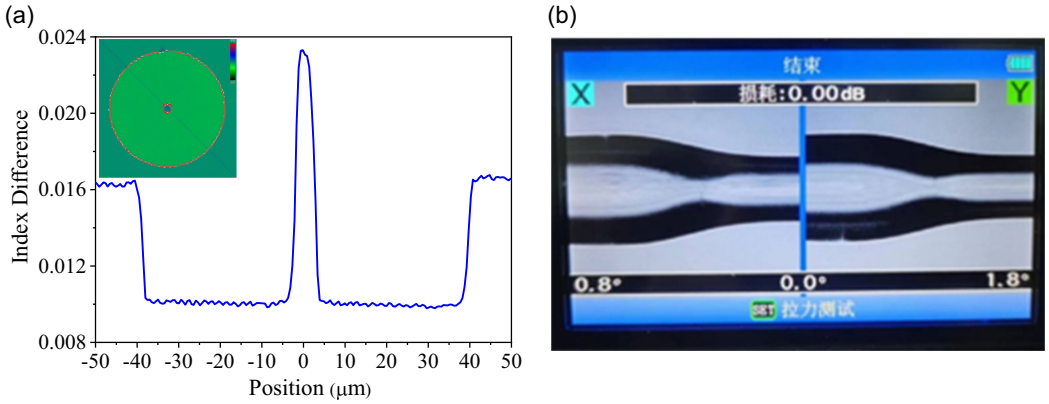

2. Literature Review

Li and Ding [19] proposed knot resonator in the microfiber and MF to create an optical magnetic field sensor, and the sensor wavelength responses linearly to the applied magnetic field. When the magnetic intensity was 60 mT, the wavelength shift up to 100 pm was achieved. The work reported in Gao et al. [20] stuffed the pores of the PCF with liquid MF. By aligning the MF nanoparticles under the influence of an applied magnetic field, the RI difference between the PCF's core and cladding can be altered. The magnetic field measurement with a resolution of 0.009 mT was achieved. An optical fiber magnetic field sensor utilizing the MF packed LPFG was proposed by Zhang et al. [21] with a sensitivity of 1.54 dB/mT in the magnetic intensity range from 0 to 0.74 mT. Li et al. [22] fabricated a magnetic field sensor according to the principle of optical polarization modulation of microfiber coated by MF. By immersing the microfiber in the MF, the optical polarization detection was used to track the magnetic field's direction and strength. Sang et al. [23] demonstrated an optical magnetic field sensor consists of a cladding-etched LPFG coated with MF and encapsulated in a capillary. The cladding-etched LPFG has dual dips, which move in the opposite wavelength direction with the changes of the magnetic field. By detecting the wavelength difference between two dips, the magnetic field was measured with a sensitivity of 0.408 nm/mT in the intensity range of 0~12 mT. Jiang et al. [18] demonstrated a vector magnetic field sensor using the MF-encapsulated LPFG inscribed in the polarization-maintaining fiber. Thanks to the fast development of MF nanoparticles, the MF-encapsulated fiber magnetic field sensors could have better sensing performance.

3. Sensor Design and Experiments

3.1. Grating fabrication

The LPFGs can be inscribed using different techniques including ultraviolet light writing method, arc discharge method, carbon dioxide laser writing method, and femtosecond laser writing method. Compared with other methods, the carbon dioxide laser writing method has the advantages that the fabricated LPFGs have good thermal stability and can be inscribed in any kinds of optical fibers.

We fabricated the LPFGs in a thin-cladding fiber (TCF) using a carbon dioxide laser. The average power of the laser is ~0.6 W. The laser scanning is controlled by computer program. By changing the grating period, the LPFGs with different order cladding modes can be inscribed in the TCF. The LPFG couples the light from fundamental core mode to high order cladding modes. The stronger evanescent field can be excited by the TCF–LPFGs, which have much smaller cladding diameter, so the grating can be more sensitive to the changes of surrounding RI than that of the conventional LPFGs. Figure 1(a) shows the measured index distribution of the TCF cross-section using a RI profiler (S14, Photon Kinetics), and the inset shows the microscopic view of the TCF. As shown in Figure 1(a), the cladding diameter, the core diameter, and the RI difference between fiber core and cladding are 5.6 μm, 80 μm, and 0.012, respectively, for the TCF used in the experiments.

In experiments, the transmission spectra of the LPFGs were measured by the system, which consists of a broadband supercontinuum light source (NKT Photonics) and an optical spectrum analyzer (OSA, AQ 6375, YOKOGAWA). To measure the transmission spectra real time, the two ends of the TCF were connected with single-mode fiber (SMF) by a commercial fusion splicer. The fusion splicing pictures of the TCF and SMF are shown in Figure 1(b). The length of the TCF for the fabrication of the LPFG is 5 cm, which constitutes the fiber structure of SMF–TCF–SMF (STCS), as shown in Figure 2. When the light beam enters the TCF at the incident end of the SMF, part of the beam is coupled into the core and the other part is coupled into the cladding of the TCF due to the mismatch of the mode field diameters of SMF and TCF. After the light transmits in both core and cladding of the TCF, part of beam in the TCF cladding is coupled back to the core area of the output SMF and interferes with the light transmitted in the TCF core, which is ultimately

Figure 2
Schematic diagram of the STCS structure

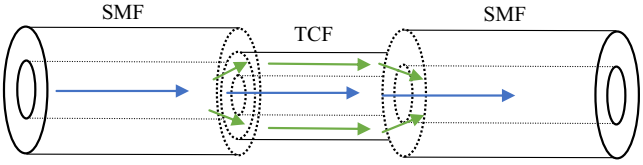

Figure 3
Transmission spectra of the TCF–LPFG with a period of 280 μm. (a) Experimental transmission spectrum. (b) Simulated transmission spectrum

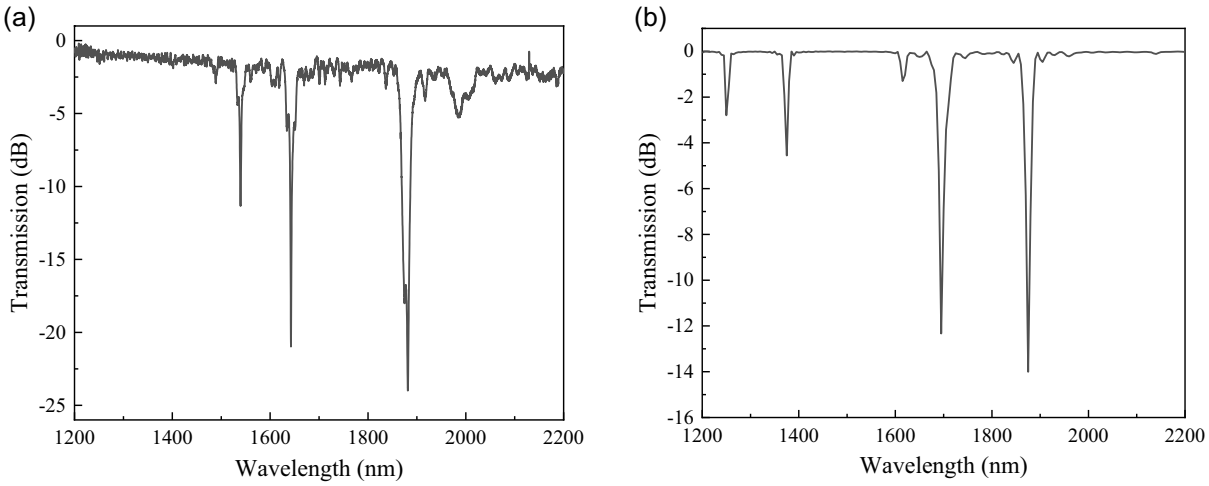

Figure 4
RI sensing characteristics of TCF–LPFG. (a) Transmission spectra of TCF–LPFG at different refractive indexes. (b) Variation of wavelength shift on surrounding RI

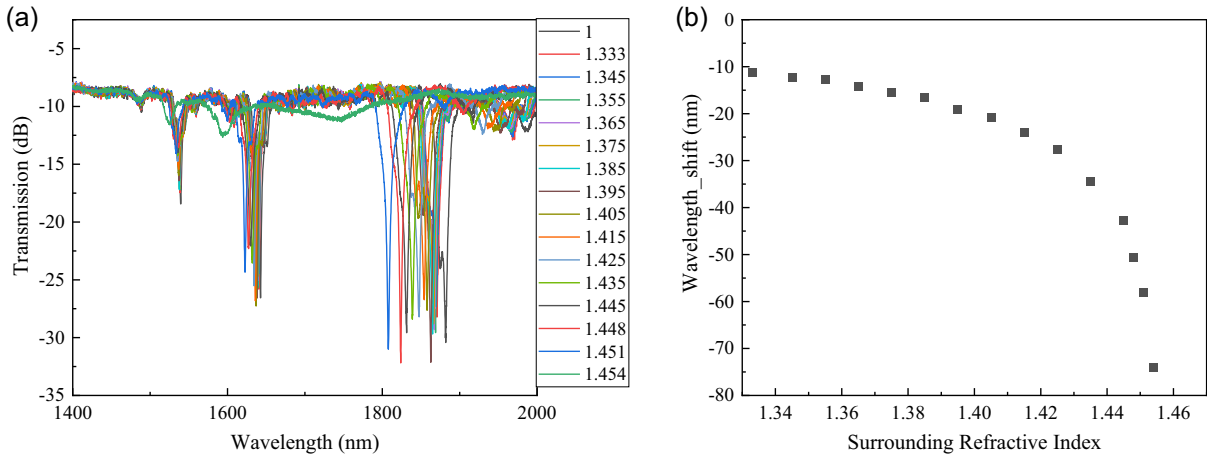

coupled into the SMF at the output end. Therefore, the STCS fiber structure forms a fiber-type Mach–Zehnder interferometer. In the experiments, the length of the fused TCF is short and the fusion points are gently connected, so the interference has no effect on the spectral measurement of the TCF–LPFGs.

The LPFGs were inscribed in the TCF by the carbon dioxide laser. The grating period is 280 μm and period number is 50. By repeating the laser scanning cycles, the LPFG with high grating contrast can be written in the TCF. Figure 3 shows the experimental and simulated transmission spectra of the TCF–LPFG with a grating period of 280 μm. According to the phase matching condition of the LPFGs, the resonance wavelength of the LPFG is $\lambda = (n_1 - n_2)\Lambda$, where Λ is the period of the TCF–LPFG, and n_1, n_2 represent the effective RI of the fundamental LP_{01} mode and the high order cladding mode, respectively. We use Rsoft software to calculate the transmission spectrum of TCF–LPFG theoretically. The difference of transmission spectra consists of interference caused by mismatch in core diameter between TCF and SMF. The resonance wavelength and mode order of the cladding mode can be given according to the simulated phase matching curve. The resonance dip around the wavelength of 1881 nm can be determined to be LP_{05} mode according to the phase matching curves.

The RI sensing characteristics of the fabricated TCF–LPFGs were investigated in the experiment. Figure 4(a) shows the transmission spectra of the TCF–LPFG with different surrounding RI. The initial wavelength of the resonance dip was measured to be ~1881 nm in air. With the increasing surrounding RI, the resonance dip shifts toward the shorter wavelength, as did the conventional LPFGs. Figure 4(b) shows the dependence of the

resonance wavelength shift on the surrounding RI. When the surrounding RI changes from 1.000 to 1.454, the maximum wavelength shift was measured to be 80 nm. A linear fit of the scatter plot of wavelength shift versus surrounding RI over the range of 1.445–1.454 yields a surrounding RI sensitivity of 3366 nm/RIU.

3.2. MF nanoparticle encapsulation of LPFG

MF is a special kind of nanostructured material that a colloid is composed of surfactants and magnetic particles. The magnetic nanoparticles are uniformly distributed in the base fluid (organic solvent or water), which is widely used in optical fiber magnetic field detection due to the tunable properties. With the applied magnetic field, the nanoparticles in the MF will change from random uniform distribution to aggregation and formation of chain structure along the magnetic field, which changes the RI of the MF. By coating the LPFG with MF liquid, the external magnetic field could be measured based on the wavelength measurement of the coated TCF–LPFG.

In experiment, a capillary tube of 2.0 mm inner diameter is used to encapsulate the LPFG with the MF. The MF is a commercial product (Ferrotec, EMG 605). The MF appears black–brown fluid composed of 10 nm particles and water. Firstly, the TCF–LPFG was placed in the axial position of the quartz capillary tube, and the MF was introduced into the tube. Then both ends of the tube were encapsulated with UV glue. A small strain was applied on the LPFG to keep the fiber in straight during the packaging. Figure 5 shows the transmission spectrum of TCF–LPFG packaged with MF in the red solid line. The black line shows the transmission spectrum of the TCF–LPFG before encapsulation for comparison. The resonance wavelength is blue-shifted by 21 nm after the TCF–LPFG encapsulated with MF. The change of resonance wavelength before and after encapsulation can be attributed to the variations of the surrounding RI due to MF coating. By comparing with the RI characteristics of the TCF–LPFG, the RI of the MF is estimated to be about 1.39. The wavelength shift due to the MF encapsulation is consistent with the RI characteristics of the TCF–LPFG.

Figure 5
Variation of transmission spectra of the TCF–LPFG before and after packaging

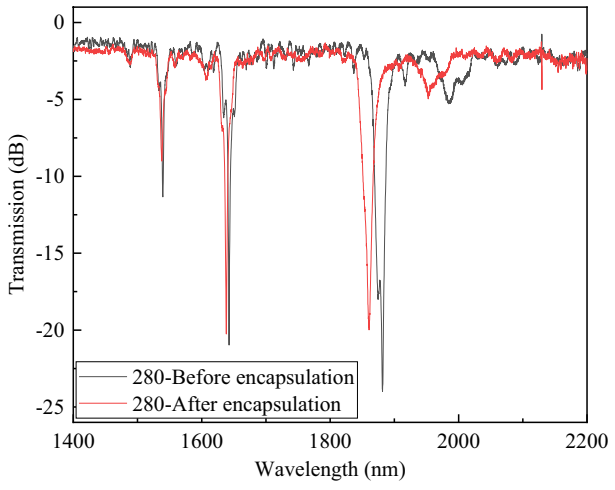

3.3. Magnetic field response characteristics

Figure 6 shows the schematic diagram of the experimental setup. An image of the packaged sensor is shown in the inset of the figure, which consists of TCF–LPFG, MF, UV-glue, and capillary tube. The encapsulated TCF–LPFG is placed horizontally at the center of the uniform magnetic field between the two magnetic poles of solenoids, so that the applied magnetic field acts perpendicularly on the LPFG. By changing the output voltage of the regulated power, the intensity of the generated magnetic field can be controlled. Therefore, the sensor can be designed for the sensing measurement of the magnetic field or the electrical current applied on the solenoids. The magnetic field intensity can be measured around the sensor head by using a Tesla magnetometer. Finally, the transmission spectra of the coated TCF–LPFG were measured by the OSA real time when the electrical current applied on the solenoids; thus, the external magnetic field around the sensor head was changed.

Figure 6
Schematic diagram of magnetic field sensing

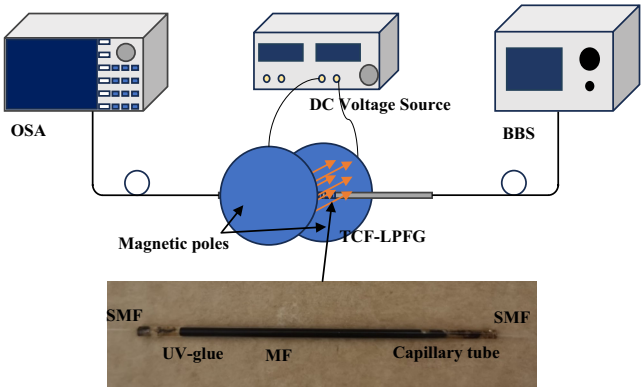

Figure 7(a) shows the transmission spectra of the TCF–LPFG when the applied magnetic field around the sensor head is changed. In the intensity range from 0 to 11 mT, the resonance dip shifts toward shorter wavelength direction, and when the maximum offset is reached, the resonance wavelength no longer shifts and tends to be constant. Figure 7(b) shows the dependence of the wavelength shift of the coated TCF–LPFG on the intensity of external magnetic field. The response of the MF-encapsulated TCF–LPFG is not completely linear. In the intensity range of 0–11 mT, a high sensitivity of 0.31 nm/mT was achieved, as shown in the figure. When the intensity of the magnetic field is larger than 11 mT, the resonance wavelength of the TCF–LPFG remains unchanged. The wavelength shift of the TCF–LPFG is affected by the RI changes induced by the aggregation and formation of chain structure of magnetic nanoparticles in MF. The magnetic nanoparticles motion reaches saturation when the applied magnetic field exceeds 11 mT.

To verify the reliability and repeatability of the sensor, we fabricate more TCF–LPFGs and encapsulate them with MF. All of them have a linear relationship between magnetic intensity and resonance wavelength. In Figure 8, different symbols represent the magnetic field response of three TCF–LPFG sensors. The experimental results show that the TCF–LPFG packaged with MF has good reliability and repeatability.

Figure 7
Magnetic field characteristics of the MF-packaged TCF–LPFG. (a) Transmission spectra with different magnetic intensity. (b) Wavelength shift at different magnetic intensity

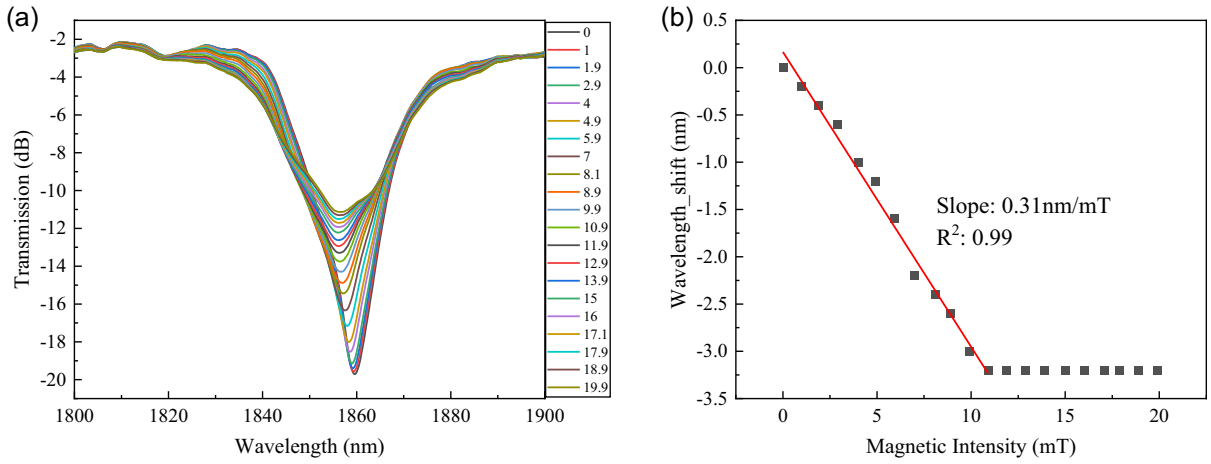

Figure 8
Reliability and repeatability of MF-encapsulated TCF–LPFGs

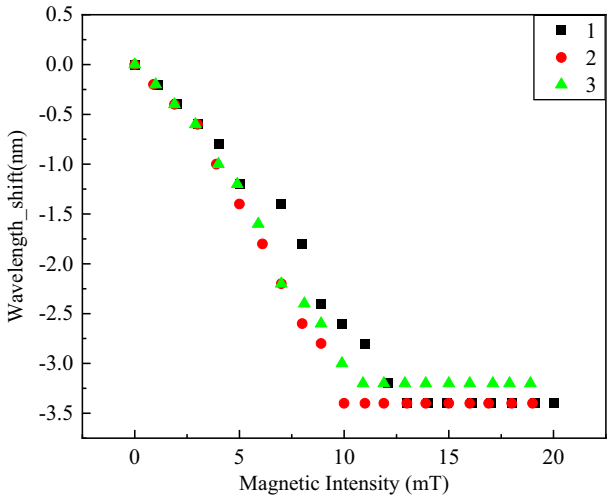

4. Conclusion

In conclusion, we demonstrated experimentally an optical fiber magnetic field sensor using the MF encapsulated TCF–LPFG. The LPFGs were inscribed in the TCF using a carbon dioxide laser, and the RI sensing characteristics of the gratings were investigated. The fabricated magnetic field sensor achieved a sensitivity of 0.31 nm/mT in the intensity range of 0–11 mT due to the high RI sensitivity of the TCF–LPFG. The fiber magnetic field sensor based on TCF–LPFGs is more sensitive than the conventional LPFG-based magnetic field sensors, which has potential applications in practical measurement of magnetic field (electrical current).

Funding Support

This work was sponsored by Science and Technology Foundation of State Grid Corporation of China No. 521835200038.

Ethical Statement

This study does not contain any studies with human or animal subjects performed by any of the authors.

Conflicts of Interest

The authors declare that they have no conflicts of interest to this work.

Data Availability Statement

Data available on request from the corresponding author upon reasonable request.

Author Contribution Statement

Hua Wang: Conceptualization, Formal analysis, Writing – original draft, Writing – review & editing, Supervision, Project administration, Funding acquisition. **Qun He:** Investigation, Resources. **Shuai Yuan:** Data curation. **Wei Zeng:** Methodology. **Yang Zhou:** Software, Resources. **Ruchao Tan:** Validation, Visualization. **Xiaolong Fan:** Writing – review & editing. **Yuehui Ma:** Writing – review & editing. **Yu Zhu:** Supervision.

References

[1] Roy, A., Sampathkumar, P., & Anil Kumar, P. S. (2020). Development of a very high sensitivity magnetic field sensor based on planar Hall effect. *Measurement*, *156*, 107590. https://doi.org/10.1016/j.measurement.2020.107590

[2] Fetisov, Y. K., Bush, A. A., Kamentsev, K. E., Ostashchenko, A. Y., & Srinivasan, G. (2006). Ferrite-piezoelectric multilayers for magnetic field sensors. *IEEE Sensors Journal*, *6*(4), 935–938. https://doi.org/10.1109/JSEN.2006.877989

[3] Li, Y., Yuan, J., Wang, Z., Song, J., & Xiao, G. (2013). Modeling of magnetic fields for application in nuclear magnetic resonance gyroscopes. In *Proceedings of 2013 2nd International Conference on Measurement, Information and Control*, *1*, 36–40. https://doi.org/10.1109/mic.2013.6757911

[4] Zhang, F., Li, B., Chen, X., Gao, Y., Yan, X., Zhang, X., . . . , & Cheng, T. (2022). A magnetic field sensor based on birefringence effect in asymmetric four-hole fiber. *Journal of Lightwave Technology*, *40*(8), 2594–2600. https://doi.org/10.1109/jlt.2021.3135271

[5] Chiavaioli, F., Baldini, F., Tombelli, S., Trono, C., & Giannetti, A. (2017). Biosensing with optical fiber gratings. *Nanophotonics*, *6*(4), 663–679. https://doi.org/10.1515/nanoph-2016-0178

[6] James, S. W., Korposh, S., Lee, S. W., & Tatam, R. P. (2014). A long period grating-based chemical sensor insensitive to the influence of interfering parameters. *Optics Express*, *22*(7), 8012–8023. https://doi.org/10.1364/oe.22.008012

[7] Layeghi, A., & Latifi, H. (2018). Tunable ferrofluid magnetic fiber sensor based on nonadiabatic tapered Hi-Bi fiber in fiber loop mirror. *Journal of Lightwave Technology*, *36*(4), 1097–1104. https://doi.org/10.1109/jlt.2017.2781623

[8] Zhang, L., Pan, J., Zhang, Z., Wu, H., Yao, N., Cai, D., . . . , & Tong, L. (2020). Ultrasensitive skin-like wearable optical sensors based on glass micro/nanofibers. *Opto-Electronic Advances*, *3*(3), 190022. https://www.oejournal.org/article/doi/10.29026/oea.2020.190022

[9] García-Miquel, H., Barrera, D., Amat, R., Kurlyandskaya, G. V., & Sales, S. (2016). Magnetic actuator based on giant magnetostrictive material Terfenol-D with strain and temperature monitoring using FBG optical sensor. *Measurement*, *80*, 201–206. https://doi.org/10.1016/j.measurement.2015.11.035

[10] Li, Y., Pu, S., Hao, Z., Yan, S., Zhang, Y., & Lahoubi, M. (2021). Vector magnetic field sensor based on U-bent single-mode fiber and magnetic fluid. *Optics Express*, *29*(4), 5236–5246. https://doi.org/10.1364/oe.416187

[11] Liu, Y., Chiang, K. S., & Chu, P. L. (2004). Multiplexing of temperature-compensated fiber-Bragg-grating magnetostrictive sensors with a dual-wavelength pulse laser. *IEEE Photonics Technology Letters*, *16*(2), 572–574. https://doi.org/10.1109/lpt.2003.822254

[12] Luo, L., Pu, S., Tang, J., Zeng, X., & Lahoubi, M. (2015). Highly sensitive magnetic field sensor based on microfiber coupler with magnetic fluid. *Applied Physics Letters*, *106*(19), 193507. https://doi.org/10.1063/1.4921267

[13] Zhang, F., Li, B., Sun, Y., Liu, W., Yan, X., Zhang, X., . . . , & Cheng, T. (2021). A magnetic field sensor utilizing tellurite fiber-induced Sagnac loop based on Faraday rotation effect and Fresnel reflection. *IEEE Transactions on Instrumentation and Measurement*, *70*, 1–7. https://doi.org/10.1109/tim.2021.3082275

[14] Yang, S. Y., Chieh, J. J., Horng, H. E., Hong, C. Y., & Yang, H. C. (2004). Origin and applications of magnetically tunable refractive index of magnetic fluid films. *Applied Physics Letters*, *84*(25), 5204–5206. https://doi.org/10.1063/1.1765201

[15] Zahn, M. (2001). Magnetic fluid and nanoparticle applications to nanotechnology. *Journal of Nanoparticle Research*, *3*(1), 73–78. https://doi.org/10.1023/a:1011497813424

[16] Das, P., Colombo, M., & Prosperi, D. (2019). Recent advances in magnetic fluid hyperthermia for cancer therapy. *Colloids and Surfaces B: Biointerfaces*, *174*, 42–55. https://doi.org/10.1016/j.colsurfb.2018.10.051

[17] Yin, J., Ruan, S., Liu, T., Jiang, J., Wang, S., Wei, H., & Yan, P. (2017). All-fiber-optic vector magnetometer based on nano-magnetic fluids filled double-clad photonic crystal fiber. *Sensors and Actuators B: Chemical*, *238*, 518–524. https://doi.org/10.1016/j.snb.2016.07.100

[18] Jiang, C., Liu, Y., Mou, C., Wen, J., Huang, S., & Wang, T. (2022). Fiber vector magnetometer based on polarization-maintaining fiber long-period grating with ferrofluid nanoparticles. *Journal of Lightwave Technology*, *40*(8), 2494–2502. https://doi.org/10.1109/JLT.2022.3140867

[19] Li, X., & Ding, H. (2012). All-fiber magnetic-field sensor based on microfiber knot resonator and magnetic fluid. *Optics Letters*, *37*(24), 5187–5189. https://doi.org/10.1364/OL.37.005187

[20] Gao, R., Jiang, Y., & Abdelaziz, S. (2013). All-fiber magnetic field sensors based on magnetic fluid-filled photonic crystal fibers. *Optics Letters*, *38*(9), 1539–1541. https://doi.org/10.1364/OL.38.001539

[21] Zhang, N. M. Y., Dong, X., Shum, P. P., Hu, D. J. J., Su, H., Lew, W. S., & Wei, L. (2015). Magnetic field sensor based on magnetic-fluid-coated long-period fiber grating. *Journal of Optics*, *17*(6), 065402. https://doi.org/10.1088/2040-8978/17/6/065402

[22] Li, X., Ma, R., & Xia, Y. (2018). Magnetic field sensor exploiting light polarization modulation of microfiber with magnetic fluid. *Journal of Lightwave Technology, 36*(9), 1620–1625. https://doi.org/10.1109/JLT.2017.2785300

[23] Sang, J., Gu, Z., & Ling, Q. (2017). Characteristics of dual-peak resonance in a tilted long-period fiber grating sensing film sensor. *Journal of the Optical Society of America B*, *34*(11), 2358–2366. https://doi.org/10.1364/JOSAB.34.002358

How to Cite: Wang, H., He, Q., Yuan, S., Zeng, W., Zhou, Y., Tan, R., Fan, X., Ma, Y., & Zhu, Y. (2024). Magnetic Field Sensor Using the Magnetic Fluid-Encapsulated Long-Period Fiber Grating Inscribed in the Thin-Cladding Fiber. *Journal of Optics and Photonics Research*. https://doi.org/10.47852/bonviewJOPR32021689